Study of De-protection Reactions for Chemically Amplified Resists

Atsushi Sekiguchi, Yoshiyuki Kono and Yoshihisa Sensu

Litho Tech Japan Corp., 2-6-6 Namiki, Kawaguchi, Saitama 332-0034, Japan

An existing FT-IR spectrometer system incorporating a bake plate for *in situ* observation of protection group removal reactions (de-protection reactions) of chemically amplified resists is modified, leading to the development of a new de-protection reaction model. Modifications to the FT-IR spectrometer system are made to ensure full contact between a wafer and the bake plate, as is the case in actual PEB systems. Processes during initial wafer heating are found to be different to the previous equipment, in which a gap of 0.2 mm existed between the wafer and baking plate. Because the results of the improved system disagree with a previous model, a new model which fits the observed data much more consistently is proposed. The new de-protection reaction model incorporates the effects of acid evaporation, which are found to be significant.

Keywords: chemically amplified resist, de-protection reaction, protection group, FT-IR spectrometer equipment, activation energy

1. Introduction

Chemically amplified resists employing acid catalysts were first researched in 1987 by Ito and coworkers [1], and have since become indispensable in the manufacture of semiconductor devices having design rules of under one-half micron. During this period, a variety of research has been conducted with aims such as increasing the resolution of chemically amplified resists and enhancing stability over a wider range of environments [2-4]. Positive tone chemically amplified resists generate acid from photo-acid generators (hereafter "PAG") through photochemical reactions, and in the heating process performed following exposure (post-exposure bake, hereafter "PEB") these acids act as catalysts in the removal of protection groups [1]. Consequently, an accurate grasp of de-protection reactions is essential in efforts to develop resists and optimize fabrication processes. In light of this, the authors have conducted studies on methods for analyzing de-protection reactions during PEB[5-8].

The FT-IR spectrometer with bake plate system described previously is improved by modifying the contact-baking apparatus so as to more closely reproduce conditions in commercial PEB systems. In addition, a new de-protection reaction model is studied. In the previous system, a gap of approx. 0.2 mm was maintained between the wafer and bake plate when positioning the wafer on the bake plate [5]. In actual PEB equipment, however, baking is performed with the wafer and substrate in contact, so that in the de-protection reaction analysis equipment of the previous report (hereafter "the previous equipment"), increases in wafer temperature during baking differ from those in the actual baking process. The experimental system was therefore improved by changing the construction so that the wafer is pressed onto the bake plate by a wafer-restraining rod as it is inserted, to ensure good physical contact. Temperature increases similar to those found in actual PEB processes could then be reproduced. However, this also revealed that the de-protection reaction model described in the previous report [5] does not adequately represent the true de-protection reaction during PEB. A new de-protection reaction model that includes the effects of acid evaporation is proposed.

2. Hardware Modifications

Figure 1 shows a schematic of the baking components of the previous equipment and of the improved experimental setup. In the previous

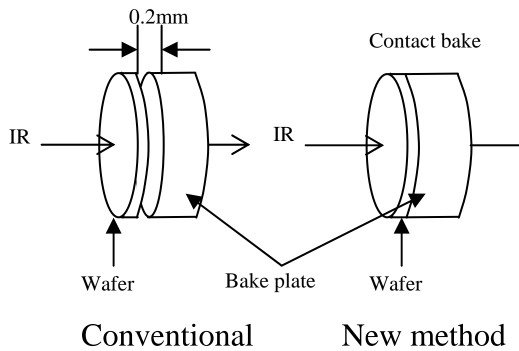

Fig. 1 The comparison of conventional bake system and new method.

equipment, a gap of approximately 0.2 mm existed between the back surface of the wafer and the baking surface while a wafer was being moved onto the bake plate using the wafer shuttle. In addition, this gap was not uniform over the wafer surface. The setup is thus improved by using a wafer-restraining rod to ensure contact between the baking plate and the wafer as the wafer is inserted, allowing contact baking to take place. Figure 2 shows photos of the improved experimental setup. The photo on

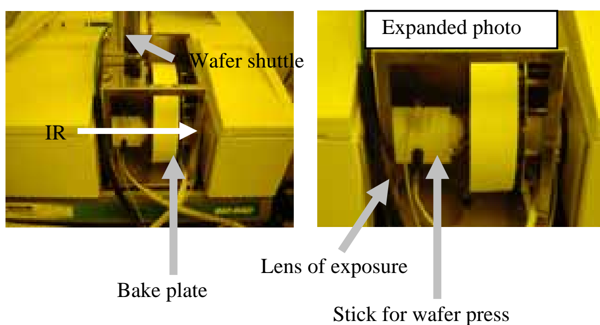

Fig. 2 External view of FT-IR and exposure bake system.

the right is an enlargement to show the wafer-restraining rod. To investigate reactions during exposure, light from a high-voltage mercury lamp (full width at half maximum of 12 nm, illuminance at the wafer surface of 1.0 mW/cm^2) was passed through a 248 nm filter before irradiating the wafer surface. A comparison of the change in wafer surface temperature with time between the previous and improved setups is shown in Figure 3 for a bake plate temperature of 110°C. In the previous equipment, wafer surface temperature did not reach 100°C until 15 seconds after the start of baking,

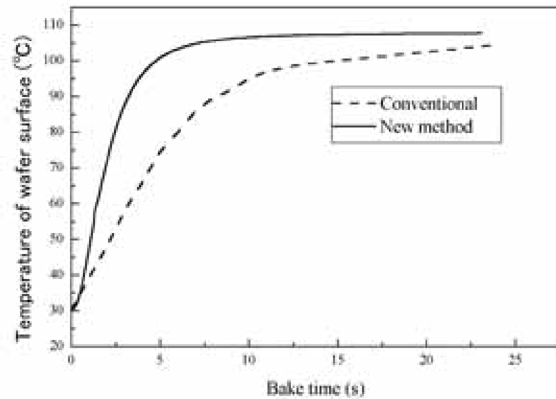

Fig. 3 Comparison of increase in temperature profile at conventional and new method.

3. Problems with the Previous Model and Study of the Spence Model

3.1 Problems with the Previous Model

De-protection reaction measurements were performed at 110°C employing positive tone chemically amplified resist based on 1-ethoxyethyl (ethyl acetal) protection groups using the improved experimental setup with the results shown in Figure 4. Also shown is the fit to the de-protection reaction model proposed previously [5], which is expressed as

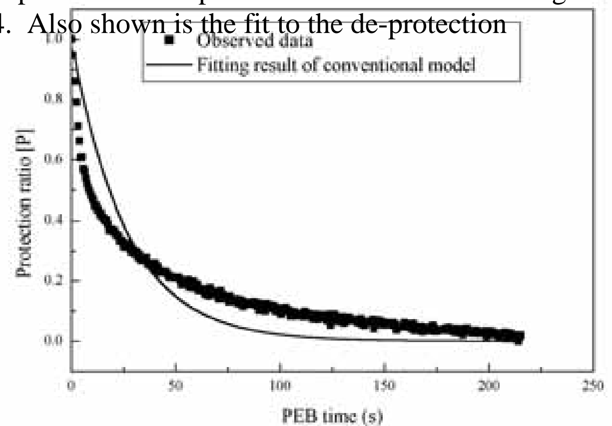

Fig. 4 Comparison of observed data and fitting result when de-protection reaction model using equation (1).

$$[P]=\exp\left[-k_{dp}\left[H^{+}\right]^{m}\left\{1-\exp\left(-\frac{m(t-T_d)}{\tau}\right)\right\}\frac{\tau}{m}\right] \quad (1)$$

$$\left[H^{+}\right] = 1 - \exp\left(-C \bullet E\right) - Q \quad (2)$$

where [P] is the normalized protection ratio of protection groups, K_{dp} is the de-protection reaction constant in PEB (s^{-1}), m is the de-protection reaction order in PEB, t is the PEB duration (s), [H] is the normalized acid concentration, C is the PAG reaction constant during exposure (cm^2/mJ), E is the exposure energy (mJ/cm^2), Q is the quenching constant, T_d is the reaction lag constant in PEB (s), and τ is the average acid lifetime in PEB (s^{-1}).

As can be seen in Figure 4, the reaction model deviates from the experimental data. This seems to be because the improved experimental setup produces faster temperature rises during the initial baking period, promoting a de-protection reaction that proceeds so rapidly that non-linearities are introduced. The reaction model does not adequately take nonlinear reaction characteristics into account, and so cannot fit the experimental data.

3.2 The Model of Spence, et al.

In 1990, C.A. Spence and coworkers categorized photochemical reactions of chemically amplified resists into acid generation reactions, de-protection reactions and acid deactivation reactions [9-11].Acid generation reactions are described as :

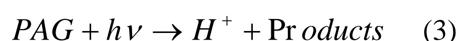

$$PAG + h\nu \rightarrow H^{+} + \Pr oducts \quad (3)$$

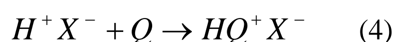

$$H^{+}X^{-} + Q \rightarrow HQ^{+}X^{-} \quad (4)$$

$$\left[H_{pag}\right] = 1 - \exp\left(-C \bullet E\right) \quad (5)$$

$$\left[H_{q}\right] = \left[H_{pag}\right] - q \quad (6)$$

where $[H_{pag}]$ is the normalized concentration of acid generated through exposure, $[H_q]$ is the acid concentration after deactivation by a quencher, C is a constant relating acid generation to exposure (cm^2/mJ), E is the exposure energy (mJ/cm^2), and q is the amount of quencher added (molar ratio with respect to PAG).

De-protection reactions are described as:

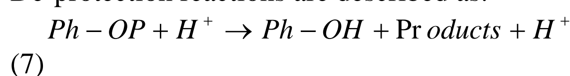

$$Ph - OP + H^{+} \rightarrow Ph - OH + \Pr oducts + H^{+}$$
(7)

$$\frac{\partial[P]}{\partial t} = -K_{dp} \bullet [P] \bullet \left[H^{+}\right]^{m} \quad (8)$$

$$[P] = P_0 \bullet \exp\left(-K_{dp} \bullet t \bullet \left[H^{+}\right]^{m}\right) \quad (9)$$

where [P] is the normalized protection group concentration, $[P_0]$ is the protection group concentration after exposure, $[H^+]$ is the normalized acid concentration, K_{dp} is the de-protection reaction constant in PEB (s^{-1}), m is the de-protection reaction order, and t is PEB duration (s).

Acid deactivation reactions are described as:

$$H^{+} \xrightarrow{K_{loss}} \quad (10)$$

$$\frac{\partial\left[H^{+}\right]}{\partial t} = -K_{loss} \bullet \left[H^{+}\right] + D\nabla^{2}\left[H^{+}\right] \quad (11)$$

$$\left[H^{+}\right] = H_{q} \bullet \exp\left(-K_{loss} \bullet t\right) \quad (12)$$

where $[H^+]$ is the normalized acid concentration, K_{loss} is the acid deactivation reaction constant (s^{-1}), and t is PEB duration (s).

The sharp bend in the de-protection curve that occurred during the initial period of PEB could not be explained using our previous reaction model. The bend in the de-protection curve represents a sharp drop in de-protection reactions in the initial PEB period, and is thought to suggest that sudden deactivation of acid occurs during the beginning of the de-protection reaction. Hence, an attempt was made to fit the data to the model of Spence et al., in which acid deactivation is represented by an acid deactivation reaction.

4. Experiments and Results

De-protection reactions at different PEB temperatures were studied using the model of Spence et al. Experimental conditions are listed in Table 1. The resist used in experiments was a

Table 1 Experimental conditions

Resist	KrF CA (EA)resist
Base polymer	PHS
Protection Group	1-Ethoxyethyl(Ethylaetal)
PAG bis(cyclohexylsulfonyl)diazomethane(BCHSDM)	

Pre-bake	110℃,90s
Thickness	700nm
Exposure	30mJ/cm^2

positive tone chemically amplified resist for KrF excimer lasers that uses 1-ethoxyethyl (ethyl acetal) protection groups (hereafter this resist is referred to as "EA resist"). Experimentally, the reaction constant C was determined by placing unexposed resist in the equipment and observing dissolution of PAG by UV exposure at room temperature (23°C). The level of de-protection during exposure was also observed, and the protection group concentration P_0 after exposure was determined using Eq. (7). The sample was then exposed to a dose of 30 mJ/cm^2 (the nominal E_{op} of this resist for 110°C PEB), and the de-protection reaction observed at a number of different PEB temperatures.

4.1 Reaction during Exposure

Figure 5 shows the reaction scheme of the de-protection reactions that occurred during PAG reaction, exposure and PEB over the course of exposure of the resist.

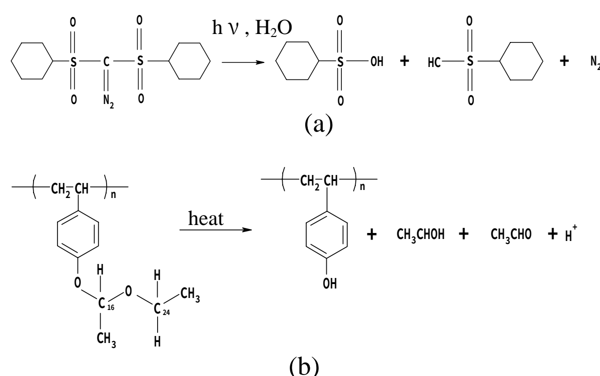

Fig. 5 Chemical structure of a chemical amplified positive resist.
(a) Chemical reaction depend on exposure and (b) De-protection reaction depend on PEB.

Bis(cyclohexylsulfonyl)diazomethane (BCHSDM), which is the PAG used in these experiments, decomposes under UV exposure and by reaction with water in the resist, generating N_2. FT-IR can be used to investigate absorption changes in azo bonds ($=N_2$) at 2150 cm^{-1} and to observe acid generation reactions caused by exposure. In de-protection reactions, however, during PEB and UV exposure, protection groups decompose through heating under acid catalysis into methanol and acetaldehyde. By using FT-IR to study absorption changes in the alkanes (H-C-H) at 2980 cm^{-1} or in ester bonds (C-O) at 950 cm^{-1}, the de-protection reaction can be observed indirectly [12]. The de-protection reaction is examined by observing absorption changes in ester bonds, as these exhibit relatively large changes in absorption. Figure 6 shows a comparison of IR absorption spectra before and after exposure to a dose of 600 mJ/cm^2. Both the absorption peak of azo bonds at 2150 cm^{-1} and the absorption peak of ester bonds at 950 cm^{-1} were found to disappear. Figure 7 shows normalized acid concentration as a function of exposure, as determined from changes

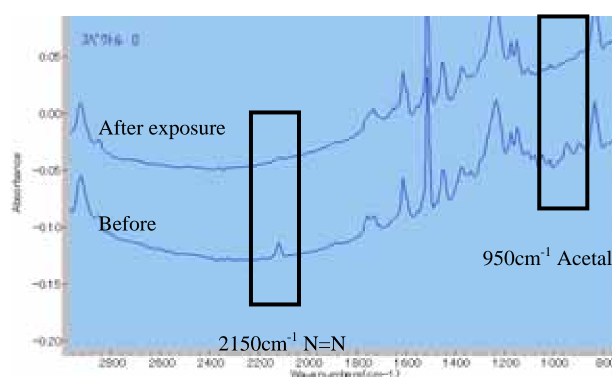

Fig. 6 The 800cm-1 to 3000cm-1 region of the infrared spectra for unexposed and exposed chemical amplified positive resist.

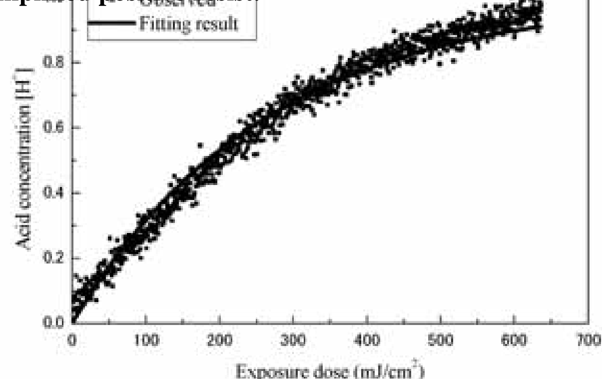

Fig. 7 Relationship between acid concentration [H$^+$] and exposure dose.

in azo bond absorption. A fit of Eq. (5) to the results is also shown, from which the reaction constant C due to resist exposure is found to be

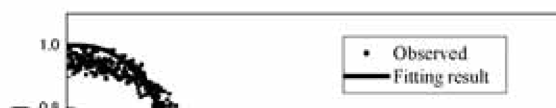

0.003778 (cm^2/mJ). Initial protection ratio as a function of exposure is shown in Figure 8, as

Fig. 8 Relationship between initial protection ratio [P_0] and exposure dose.

determined from changes in ester bond absorption. The de-protection reaction constant during exposure was calculated from the relation between exposure amount and protection group concentration after exposure, given by:

$$[P_0] = \frac{1}{\left(1 + \frac{E}{a}\right)b} \quad (13)$$

where [P_0] is the initial normalized concentration of protection groups after exposure, E is the exposure dose (mJ/cm^2), and a and b are constants.

The values of the constants were found by fitting to give a=206.55 and b=3.095, thus resulting in an initial normalized protection ratio after exposure of [P_0]=0.98 for the dose of 30 mJ/cm^2 that was used in experiments. Therefore, almost no de-protection was found to occur during exposure at the exposure dose used in this study.

4.2 De-protection Reaction during PEB

Observations of the de-protection reaction during PEB were performed by examining the 950 cm^{-1} ester bond absorption, as used in earlier measurements. Figure 9 shows IR spectra data for

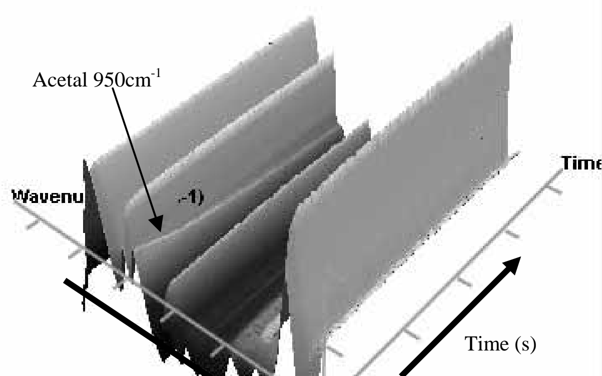

Fig. 9 Typical FT-IR difference showing de-rotection reaction as function of PEB time.

110°C PEB. It is seen that the de-protection reaction causes a gradual decrease in absorption by ester bonds with PEB duration. The relationship between PEB time and protection ratio is shown in Figure 10 for PEB temperatures from 34°C to 110°C. Results of fitting to the model of Spence et al. are also

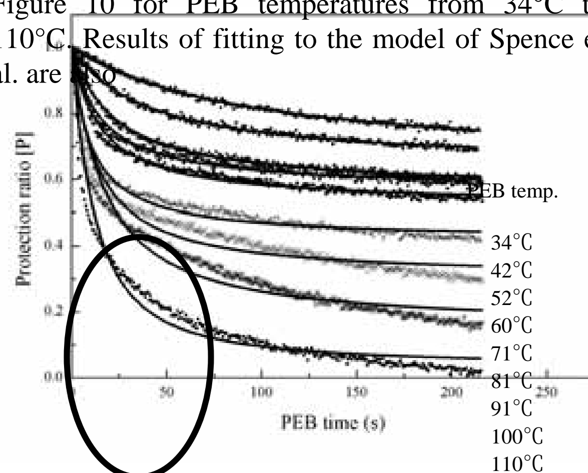

Fig. 10 Relationship between protection ratio [P] and PEB time for different PEB temperature when de-protection reaction model using equation (2).

shown. The agreement is good at relatively low temperatures from 34°C to 60°C, but in the high-temperature region of 71°C to 110°C, deviations immediately after baking begins become evident.

5. Proposal of a New De-protection Reaction Model and Analysis of De-protection Reactions

Although the results of fitting using the model of Spence et al. [10] were in good agreement at the comparatively low temperatures of 34°C to 60°C, in the high-temperature range of 71°C to 110°C deviations from the experimental results become prominent, particularly immediately following the commencement of baking. In the initial baking

period, the wafer temperature is believed to rise rapidly so that the de-protection reaction occurs suddenly, with acid deactivation and acid evaporation also abruptly beginning at the same time. This tendency is found to become more pronounced at higher temperatures. Although the effect of acid deactivation is taken into account in the model of Spence et al., acid deactivation reactions are known to be effected in complex ways by the decrease in acid levels accompanying the thermal diffusion of quenchers, the lifetime of the acid itself, and the effects of acid evaporation. The acid generated from the PAG used in these experiments is sulfonic acid, and evaporates comparatively easily. Such easily evaporated acid is expected to evaporate particularly abruptly during the initials baking stages due to the rapid rise in the wafer temperature, with the behavior of the reaction expected to be markedly different to acid lifetime or other effects. Acid deactivation components in the model of Spence and coworkers were thus divided into an acid evaporation components and an acid deactivation component, and a new model constructed. The new model (called the LTJ model) is as follows:

$$\left[H^{+}\right]=\frac{H_{q}}{\left\{K_{loss}\bullet t\bullet\exp\left(-K_{eva}\bullet t\right)+1\right\}} \quad (14)$$

where $[H^{+}]$ is the normalized acid concentration, K_{loss} is the acid deactivation reaction constant (s^{-1}), K_{eva} is the acid evaporation reaction constant (s^{-1}), and t is PEB duration (s).

Figure 11 shows the results of fitting to the LTJ model. A very good fit was obtained over the entire temperature range. Table 2 shows fitting parameters of the LTJ model along with RMS deviation values.

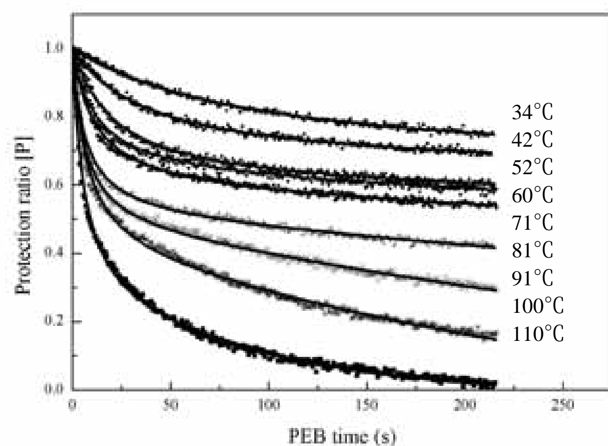

Fig. 11 Relationship between protection ratio [P] and PEB time for different PEB temperature when de-protection reaction model using equation (3).

Table-2 Fitting result of LTJ model.

Temp(°C)	$K_{dp}(s^{-1})$	$K_{loss}(s^{-1})$	$K_{eva}\times10^{-4}(s^{-1})$	RMS
34	0.0344	0.0084	0.10	0.01148
42	0.8108	0.0203	0.99	0.01617
52	0.1740	0.0351	2.18	0.02112
60	0.2893	0.0635	6.57	0.02590
71	0.3332	0.0634	6.49	0.04343
81	0.7060	0.1081	11.53	0.04719
91	0.8119	0.1095	22.17	0.08213
100	0.9002	0.1127	34.02	0.08954
110	1.1719	0.1263	52.16	0.03881

As an example, reaction constants of the deprotection, acid deactivation and acid evaporation reactions are 1.17190 (s^{-1}), 0.1265 (s^{-1}) and 0.0052 (s^{-1}) at 110°C; the reaction rate of the acid evaporation reaction is thus only 0.44% of that of the de-protection reaction. As good fits to the experimental data were obtained using the model, an attempt to determine activation energies and acid diffusion constants was made by plotting the reaction constants in the Arrhenius plot shown in Figure 12. Activation energies and acid diffusion

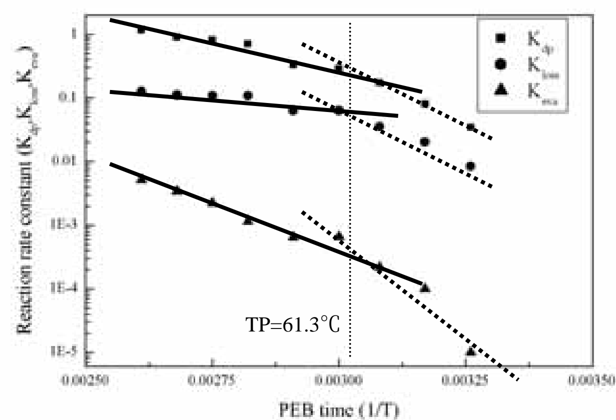

Fig. 12 Arrhenius plot.

constants were computed by applying the model of Jeffrey Byers, John Petersen et al. (the Byers-Petersen model) [13-16] to both de-protection reaction rates and the extended form of that model (Byers-Petersen extended model) to computation of acid deactivation reaction rates and acid evaporation reaction rates.

Byers-Petersen Extended Model

De-protection reaction:

$$\frac{\partial[P_{amp}]}{\partial t} = -K_{dp} \bullet [H^+] \bullet [M] \quad (15)$$

$$K_{dp} = \frac{K_{amp} \bullet K_{amp-diff} \bullet D_{amp}}{K_{amp} + K_{amp-diff} \bullet D_{amp}} \quad (16)$$

$$K_{amp} = Ar_{amp} \bullet \exp\left(-\frac{Ea_{amp}}{RT}\right) \quad (17)$$

$$K_{amp-diff} = Ar_{amp-diff} \bullet \exp\left(-\frac{Ea_{amp-diff}}{RT}\right) \quad (18)$$

$$D_{amp} = Ar_{D_{amp}} \bullet \exp\left(-\frac{Ea_{D_{amp}}}{RT}\right) \quad (19)$$

Acid deactivation reaction:

$$\frac{\partial[P_{loss}]}{\partial t} = -K_{loss} \bullet [H^+] \bullet [M] \quad (20)$$

$$K_{loss} = \frac{K_{stall} \bullet K_{stall-diff} \bullet D_{stall}}{K_{stall} + K_{stall-diff} \bullet D_{stall}} \quad (22)$$

$$K_{stall} = Ar_{stall} \bullet \exp\left(-\frac{Ea_{stall}}{RT}\right) \quad (23)$$

$$K_{stall-diff} = Ar_{stall-diff} \bullet \exp\left(-\frac{Ea_{stall-diff}}{RT}\right) \quad (24)$$

$$D_{stall} = Ar_{D_{stall}} \bullet \exp\left(-\frac{Ea_{D_{stall}}}{RT}\right) \quad (25)$$

Acid evaporation reaction:

$$\frac{\partial[P_{eva}]}{\partial t} = -K_{eva} \bullet [H^+] \bullet [M] \quad (26)$$

$$K_{eva} = \frac{K_{dispa} \bullet K_{dispa-diff} \bullet D_{dispa}}{K_{dispa} + K_{dispa-diff} \bullet D_{dispa}} \quad (27)$$

$$K_{dispa} = Ar_{dispa} \bullet \exp\left(-\frac{Ea_{dispa}}{RT}\right) \quad (28)$$

$$K_{dispa-diff} = Ar_{dispa-diff} \bullet \exp\left(-\frac{Ea_{dispa-diff}}{RT}\right) \quad (29)$$

$$D_{dispa} = Ar_{D_{dispa}} \bullet \exp\left(-\frac{Ea_{D_{dispa}}}{RT}\right) \quad (30)$$

Table 3 shows the activation energies computed from Arrhenius plots of each of the reaction constants, frequency factors and diffusion coefficients. Comparison of the activations energies reveals that reaction rate determining steps for the different reaction rate constants change at 61°C. Activation energies are found to be higher in the low-temperature region than in the high-temperature region, with rates in the high-temperature region found to be limited by the acid diffusion reaction, and those in the low-temperature region limited by the reaction rate. These results support the findings of Yamana et al. [17,18]. Activation energies in the high-temperature range are 5.36 kcal/mol for the de-protection reaction itself, 3.54 kcal/mol for the acid deactivation reaction and 12.49 kcal/mol for the acid evaporation reaction. The acid evaporation reaction thus has a higher activation energy than the de-protection reaction.

Table-3 Active energy and frequency factor of de-protection reaction for difference reaction rate constant.

Reaction rate constant		Active energy Ea(kcal/mol)	Frequency factor Ar (s^{-1})
K_{dp}	High-temp. region.	5.36	7.19
	Low-temp. region	14.74	21.03
K_{loss}	High-temp. region.	3.54	2.59
	Low-temp. region	15.81	21.13
K_{eva}	High-temp. region.	12.49	11.14
	Low-temp. region	29.68	37.51

6. Summary

The FT-IR spectrometer equipment with integrated bake plate that had previously been reported by the authors [5-8] was improved by adding a contact baking construct similar to that used in actual PEB equipment, and was used to study a new de-protection model. The equipment

was modified such that a wafer-restraining rod holds the wafer firmly against the bake plate during wafer insertion to give a better reproduction of PEB conditions. In addition, as the de-protection reaction model presented in a previous report does not describe the de-protection reaction adequately, a new de-protection reaction model in which the effects of acid evaporation were incorporated was proposed. This new model, based on the model of Spence et al., was found to fit experimental data over a broad range of PEB temperatures. Reaction rate constants thus obtained were plotted in an Arrhenius plot, with the Byers-Petersen extended model applied to the calculation and comparison of activation energies. From these results, two distinct temperature ranges were confirmed to exist; a high-temperature region in which acid deactivation, acid evaporation and de-protection reaction rates are limited by acid evaporation, and a low-temperature region in which the reaction itself is the limiting factor. In addition, activation energies were found to be higher for the acid deactivation and acid evaporation reactions compared to the de-protection reaction. In future work, the effect of quenchers is also to be included in a more rigorous model.

Acknowledgements

The authors wish to thank Tamura, a senior engineer at Tokyo Ohka Kogyo Co., Ltd. for providing materials as well as useful advice through the course of this research. Gratitude also goes to Hatakeyama, a senior researcher at Shin-etsu Chemical Co., Ltd. for useful advice relating to the construction of a de-protection reaction model. Finally, thanks go to Dr. Petersen of PAL for useful discussions of de-protection reaction analysis.

References

[1] H. Ito, and C. G. Willson: ASC Symp. Ser. **2** (1984) 11.
[2] J. V. Crivello, and J. H. W. Lam: Macromolecules **10** (1977) 1307.
[3] G. Pawlowski, R. Dammel, and C. R. Lindley: Proc. SPIE **1262** (1990) 16.
[4] R. D. Allen, I. Y. Wan, G. M. Wallraff, R. A. Dipietro, and D. C. Hofer: Proc. SPIE **1262** (1990) 412.
[5] A. Sekiguchi, M. Isono and T. Matsuzawa: Jpn. J. Appl. Phys. **38** (1999) 4936.
[6] A. Sekiguchi, C. A. Mack, M. Isono, and T. Matsuzawa: Proc. SPIE **3678** (1999) 985.
[7] Y. Miyake, M. Isono, and A. Sekiguchi: Proc. SPIE **4345** (2001) 1001.
[8] Y. Miyake, M. Isono, and A. Sekiguchi: Journ. Photopolymer **14** (2001) 463.
[9] R. A. Ferguson, C. A. Spence, Y. S. Shacham-Diamand, and A. R. Neureuther: Proc. SPIE **1086**(1989) 262.
[10] R. A. Ferguson, C. A. Spence, and E. Reichmanis, L. F. Thompson, and A. R. Neureuther: Proc. SPIE **1262** (1990) 412.
[11] C. A. Spence, S. A. MacDonald, and H. Schlosser: Proc. SPIE **1262** (1990) 344.
[12] A. Sekiguchi, Y. Miyake, and M. Isono: Jpn. J. Appl. Phys. **39** (2000) 1392.
[13] J. S. Petersen, C. A. Mack, J. W. Thackeray, R. Sinta, T. H. Fedynyshyn, J. M. Mori, J. D. Byers, and D. A. Miller: Proc. SPIE **2438** (1995) 153.
[14] J. S. Petersen, C. A. Mack, J. Sturtevant, J. D. Byers, and D. A. Miller: Proc. SPIE **2438** (1995) 167.
[15] J. D. Byers, J. S. Petersen, and J. Sturtevant: Proc. SPIE **2724** (1996) 156.

[16] J. S. Petersen, J. D. Byers, and D. Drive: Proc. SPIE **2724** (1996) 163.
[17] M. Yamana, T. Itani, H. Yoshino, S. Hashimoto, N. Samoto, and K. Kasama: Proc. SPIE **3094** (1997) 269.
[18] M. Yamana, T. Itani, H. Yoshino, S. Hashimoto, H. Tanabe, and K. Kasama: Proc. SPIE **3333** (1998) 32.